

Amorphization Effects on the Basic Sites of Nanometric Magnesium Oxide

Neftalí Lenin Villarreal Carreño,^{a,*} David Keyson,^b Marcia Tsuyama Escote,^b
Edson Roberto Leite,^b Elson Longo,^b Humberto Vieira Fajardo,^{c,*} Luiz Fernando Dias Probst,^c
Antoninho Valentini,^d Miryam Rincón Joya,^e and Paulo Sergio Pizani^e

^a*Instituto de Química, DQAI, Universidade Federal de Pelotas, CP-354, CEP-96010-900, Capão do Leão, RS, Brazil*

^b*Departamento de Química, Universidade Federal de São Carlos, 13565-905, São Carlos – SP, Brasil*

^c*Departamento de Química, Universidade Federal de Santa Catarina, 88040-900 Florianópolis – SC, Brasil*

^d*Departamento de Química Analítica e Físico-Química, Universidade Federal do Ceará, 60455-760, Fortaleza – CE, Brasil*

^e*Departamento de Física, Universidade Federal de São Carlos, 13565-905, São Carlos – SP, Brasil*

RECEIVED DECEMBER 20, 2005; REVISED MAY 8, 2007; ACCEPTED JUNE 20, 2007

Keywords
magnesium oxide
amorphization
catalysts
photoluminescence
aldol condensation

The paper reports the catalytic action of the basic sites of nanocrystalline particles of rare earth-doped magnesium oxide in the aldolization reaction between acetone and methanol leading to the C–C bond formation of an α,β -unsaturated compound (methyl vinyl ketone), also forming methyl ethyl ketone and isopropyl alcohol. Undoped and doped MgO samples were prepared by high-energy mechanical milling of commercial Mg, Y and Ce oxide powders. Catalytic activity and surface basicity of these compounds were strongly influenced by doping and the time of mechanical milling (amorphization process). Such milling leads to the formation of nanocrystalline materials. Influence of mechanical processing of these compounds was investigated by means of N₂ adsorption (BET), X-ray diffraction (XRD), TEM, CO₂ chemisorption and room temperature photoluminescence emission. Strong changes of polar groups such as hydroxyl groups on the surface of the solid were directly related to the photoluminescence emission observed.

INTRODUCTION

Several catalytic processes are promoted by rare earth-doped magnesium oxides, and effects of rare earth oxide addition in the amorphization process have been also reported. Processing features of the preparation methods, such as annealing temperature and time, gas environment,

morphology and precursor sources, affect the surface uniformity of product oxides and thereby the activity of these materials.^{1–4}

The basicity and basic strength distribution (weak, strong and intermediate strength basic sites) of magnesium oxide promoted by rare earth doping are well known,

* Authors to whom correspondence should be addressed. (E-mail: neftali@ufpel.edu.br; hfajardo@qmc.ufsc.br)

but these surface properties are strongly influenced by preparation conditions, rare earth promoter and also by its concentration.^{5–8}

High-energy mechanical milling is a well-known process employed in the preparation of nanostructured metals and alloys, which has now become quite popular in ceramic materials processing.⁹ The objectives of milling include particle size reduction, mixing or blending, and particle morphology changes.¹⁰

With the aim to prepare nanostructured metal oxide, this paper presents the results observed in the high-energy mechanical milling process applied in the preparation of nanostructured MgO. To follow changes in the material properties due to the amorphization process, CO₂ adsorption and photoluminescence emission were carried out. In addition, the catalytic activity of the basic sites on the aldolization reaction between acetone and methanol, leading to the C–C bond formation for the synthesis of an α,β -unsaturated compound (methyl vinyl ketone), was monitored. This catalytic reaction can be used as a probe to evaluate changes in the catalyst surface due to the preparation process.¹¹

Catalytic syntheses of α,β -unsaturated compounds (*via* aldol condensation) are economically attractive owing to their applications as raw materials for many synthetic organic processes.¹²

EXPERIMENTAL

Sample Preparation

MgO powders (E. Merck, Germany), pure and mixed with CeO₂ or Y₂O₃ (E. Merck, Germany) at mole ratios 5:95 and 10:90, were obtained by the conventional mixed-oxide method. They were mechanically milled, using a high-energy attrition mill (Szegvari Attritor System 01HD). The rotation speed was fixed at 500 rpm, using ZrO₂ milling spheres with 2.0 mm diameter, dispersed in an isopropyl alcohol solution at room temperature. Experiments were conducted individually at the same rotation speed for different milling times (1, 20, 40 and 80 h).

Characterization

Powder characterization by X-ray diffraction (XRD) of undoped and doped MgO samples was performed in a D5000 XRD Siemens diffractometer, equipped with a graphite monochromator and using Cu-K α radiation, 2θ ranging from 10 to 75°. The measurements were performed in order to analyze the structural evolution as the time of mechanical milling was increased. For the transmission electron microscopy (TEM) study, performed using a 200 kV Model CM200 from Philips, Holland, a drop of the powder suspension was deposited on a carbon-covered nickel grid.

Photoluminescence spectra measurements were performed using a U1000 Jobin-Yvon double monochromator

coupled to a cooled GaAs photomultiplier and a conventional photon counting system. The 488 nm lines of an argon ion laser were used as excitation light. The maximum output power of the laser was kept within 200–300 mW and cylindrical lenses were used to prevent sample overheating. All measurements were taken at room temperature.

The N₂ adsorption isotherms at liquid N₂ temperature and CO₂ adsorption isotherms at 27 °C were determined with an Autosorb-1C instrument (Quantachrome Instruments, USA). Samples were first heated and degassed at 300 °C, then maintained at that temperature for 1 h. Determination of the specific surface area of the samples was done by the BET method. The amount of irreversible CO₂ uptake was obtained from the difference between the total CO₂ adsorption on the catalyst and another CO₂ adsorption series determined after evacuation of the catalyst sample for 20 minutes, at the same temperature.

Catalytic Measurements

Gas-phase catalytic vinylation of acetone to methyl vinyl ketone (MVK) was carried out in a fixed-bed continuous flow reactor made of stainless steel, at atmospheric pressure (300 °C) and loaded with 0.1 g of catalyst. Catalysts were first heated in a flow of helium up to 350 °C and then maintained at that temperature for 1 h. The reaction gas was composed of acetone and methanol in a 1:2 mole ratio. The total flow rate of the reaction gas was 60 cm³/min, with He as carrier gas. Products were analyzed by gas chromatography (SHIMADZU 14B GC instrument), with a flame ionization detector and a CBP1 column, for 4 hours time-on-stream.

RESULTS AND DISCUSSION

Crystalline Phase Characterization

Figure 1 shows the typical patterns of MgO, pure and doped with CeO₂ (mole fraction, $x = 10\%$) and Y₂O₃ ($x = 5$ and 10%), subjected to several mechanical milling times. Peaks of the samples mechanically milled for 1 hour were indexed as belonging to MgO, CeO₂ and Y₂O₃ according to the literature.¹³ The figures also display the behavior of the crystalline structure when the compounds were subjected to higher milling times, t . The evolutions were observed by the X-ray diffraction measurements taken after the period t . A typical example is shown in Figure 1a, displaying the patterns of pure MgO obtained after different milling times. First, it is important to note that the patterns for samples milled for more than 20 hours revealed not only reflections belonging to MgO but also to the additional magnesium hydroxide (Mg(OH)₂) phase formation due to the milling process (Figure 1a). Peaks of Mg(OH)₂ became more intense as t increased, and after 80 hours of milling time the XRD suggested the Mg(OH)₂ as the main phase. From these diffractograms, we have estimated the full maximum at half width FWHM of the reflection at $2\theta \approx 42^\circ$ to verify

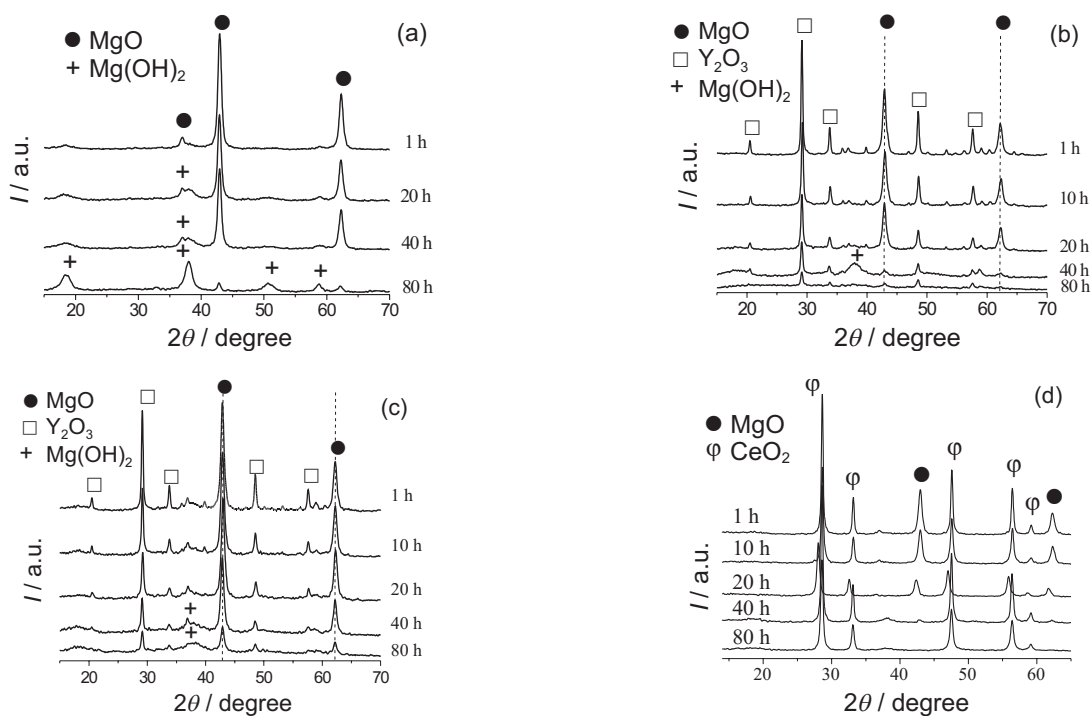


Figure 1. XRD patterns obtained from a) undoped; b) Y ($x = 10\%$), c) Y ($x = 5\%$), and d) Ce ($x = 10\%$) doped MgO powders milled for different times.

this point. We have obtained average FWHM values close to 0.6° and, using the Scherrer relation, the average grain size close to 10 nm for these samples.¹⁴

The X-ray diffraction patterns of MgO doped with Y_2O_3 and CeO_2 disclosed similar results (see Figures 1b-d). However, we have not observed the presence of the $Mg(OH)_2$ phase for the samples doped with CeO_2 . In addition, such patterns also revealed that the content of the MgO amorphous phase seemed to be related to the concentration of rare earths. In fact, comparing Figures 1b and 1c, we verify that the fraction of crystalline MgO, after 20 h of milling, was higher for the sample with 5% than for the sample with 10% of Y_2O_3 . We believe that this behavior was associated with the abrasive characteristics of the rare earth oxides.^{15,16}

Based on these data, we have calculated the lattice parameters by using the Fullprof refinement program.¹⁷ For this, we have assumed the samples to be a mixture of oxides of Mg and of R ($R = Ce$ and Y) and, in some cases, we have also added $Mg(OH)_2$.¹⁸ The values of lattice parameters obtained for MgO, $MgO-Y_2O_3$ (10%) and $MgO-CeO_2$ (10%) are listed in Table I. These values are in good agreement with those of $a = 4.21$, 10.604 and 5.411 Å reported for the MgO, Y_2O_3 and CeO_2 , respectively, in the literature.¹³

According to the experimental results and a quantum mechanics study earlier reported by several authors, water vapour is chemically adsorbed on the surface of MgO, resulting in magnesium vacancies.^{19–21} In this process, one water molecule interacts with one MgO

TABLE I. Calculated lattice parameters of MgO powders, pure and doped with Y and Ce, subjected to different times of milling

Milling time / h:		1 h	20 h	40 h	80 h
		$a / \text{Å}$			
MgO	a_{MgO}	4.214(2)	4.216(3)	4.206(4)	4.22(1)
	$a_{Mg(OH)_2}$	–	3.121	3.115	3.091
MgOY 10 % ^(a)	a_{MgO}	4.223(1)	4.223(1)	4.216(4)	4.225(3)
	$a_{Y_2O_3}$	10.617(2)	10.617(3)	10.607(7)	10.664(5)
MgOCe 10 % ^(a)	a_{MgO}	4.2222(7)	4.216(1)	4.23(1)	4.22(5)
	a_{CeO_2}	5.4157(6)	5.408(1)	5.415(1)	5.414(1)

^(a) x_Y and x_{Ce} is 10 %.

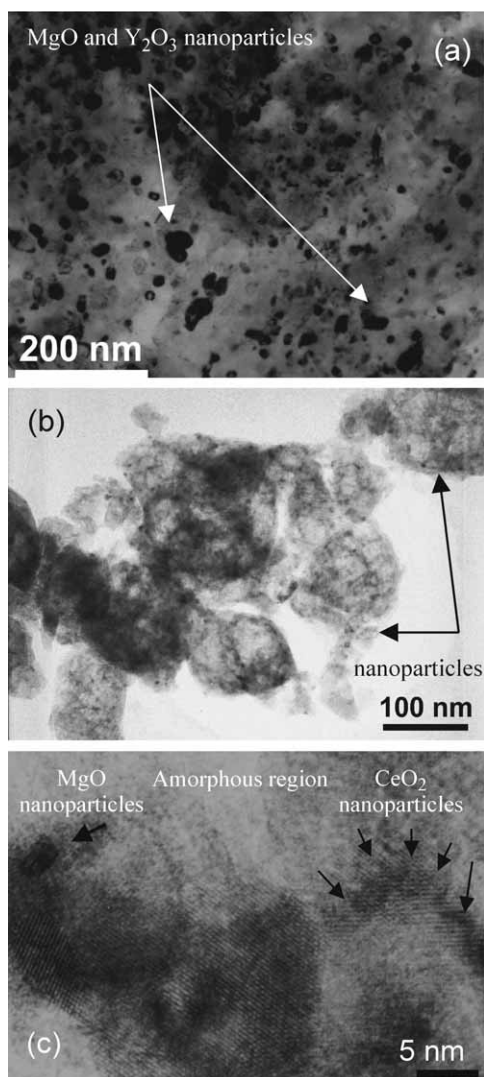


Figure 2. TEM images of MgO powders: a) Y-doped ($x_Y = 10\%$) milled for 1 h, b) Y-doped ($x = 10\%$) milled for 80 h, and HRTEM images Ce-doped ($x_{Ce} = 10\%$) milled for 40 h.

molecule, forming magnesium hydroxide. Since our powders are mechanically milled in an isopropyl alcohol solution at room temperature, such conditions would favor the process of $Mg(OH)_2$ formation. Thus, we believe that the water molecule dissociation at the active sites of the MgO crystal surface would occur more easily with the mechanical milling process, which leads to the formation of defects and vacancies on the MgO surface and the existence of OH groups adsorbed on Mg^{2+} .²²

Microstructure Characterization

Decrease in particle size was confirmed by TEM analysis. Figures 2a and b show the Bright-Field (BF) TEM images of Y-doped MgO ($x = 5\%$) milled for 1 and 80 h. Random variation in the size of nanocrystalline particles was observed. Decrease in the mean particle size upon an increase of the milling time was observed. BF-TEM

analyses also showed that the particles did not exhibit a homogeneous form. Figure 2c presents the HRTEM image of Ce-doped MgO ($x = 10\%$), milled for 40 h, illustrating the cleavage of crystalline planes (marked by dark arrows).¹⁵

Chemical Structures Characterized by Photoluminescence

It is known that crystalline oxides exhibit photoluminescence emission at low temperature (-5 to -70 °C). Recently Leite *et al.*⁹ reported intense visible photoluminescence emission at room temperature in amorphous nanostructured $PbTiO_3$ powders, prepared by the polymeric precursor method. The results pointed to the relation between the ratio of amorphous phase and the intensity of photoluminescence emission. High-energy mechanical milling can modify particle structure, resulting in localized states in an interfacial region between the crystalline and amorphous regions. The presence of these localized states is believed to be responsible for the photoluminescence emission obtained. Since the photoluminescence property is associated with the structural disorder of a solid material,²³ the presence of these localized states due to the milling process can promote the photoluminescence emission of a solid at room temperature.

The photoluminescence technique has received great attention in several characterization studies of solid surfaces.^{24–28} Therefore, the changes in properties promoted in the MgO samples due to the milling process and the influence of CeO_2 and Y_2O_3 were also followed by photoluminescence emission, at room temperature.

Figure 3 represents the photoluminescence emission spectra of undoped and Y-doped ($x = 5$ and 10%) magnesium oxide after different milling times (1, 40 and 80 h).

It shows broad photoluminescence emission spectra, which are typical of amorphous powders.^{9,29–30} The spectra exhibit maximum emissions between 515 and 540 nm, and the intensity of all samples shows their dependence on the milling time; as can be seen, Figure 3a displays negligible photoluminescence emission of the MgO starting powder (unmilled).

The mechanism that led to higher photoluminescence intensities in our samples is not clearly understood, but it may be associated with the increase of the defect center promoted by the milling process, transforming a previously crystalline structure into an amorphous system.

Addition of rare earths caused a decrease in the photoluminescence intensity of MgO; such behaviour may be attributed to charge disproportionation due to the rare earth doping.

It has been reported that the photoluminescence in MgO-based materials is related to the relaxation lumi-

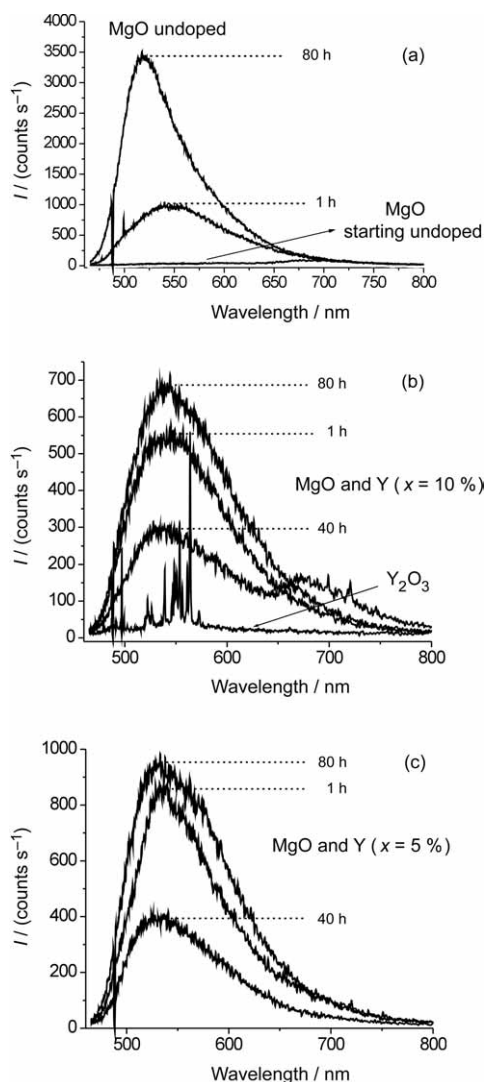


Figure 3. Photoluminescence spectra of a) undoped; b) Y ($x = 10\%$) and c) Y ($x = 5\%$) doped MgO powders subjected to different milling times.

nescence of defect centers, once the progress of cracks causes bond breaking and nuclear motion, and promotes release of atoms and ions from the lattice sites, resulting in formation of defects.^{27,28} Moreover, movement of dislocations mechanically excites the defects.

Anpo *et al.*^{31,32} studied the photocatalyzed isomerization of butene on MgO catalysts previously degassed at high temperature. These catalysts exhibit photoluminescence at 340–450 nm, which was associated with coordinatively unsaturated surface ions. The authors' results suggest a correlation between the photoluminescence response and the coordination number of oxygen ions.

In the past decade, Kawaguchi³³ reported the effect of OH content on the fractoluminescence and photoluminescence spectra of silica glasses. This author also discussed the formation and excitation processes of oxygen deficient centers (responsible for the luminescence

observed), and especially the role of hydroxyl groups on the cleavage of silica bonds. These observations indicated dependence of the photoluminescence intensity on the amount of hydroxyl groups. In another study, Yoshida *et al.*³⁴ investigated the photoluminescence emission spectra from hydroxyl groups on magnesium oxide, which were centered at 520 nm. These hydroxyl groups are directly related to photoluminescence emission and can mask the emission from Mg-O ion pairs on the surface. Properties of hydroxyl groups on the surface may also be influenced by the coordination state. The type of coordination affects the surface properties, such as basicity and surface band-gap.^{34,35}

Increase and decrease in the intensity of photoluminescence are correlated with small electronic and structural perturbations in the chemical surroundings of MgO active sites, which are strongly affected by the milling process.

Chemisorption of CO₂

Recently, Varga *et al.*⁴ reported a promising catalytic application of copper oxide dispersed in MgO by mechanical milling. This material exhibited high basicity values, parallel with the MgO content of samples and milling time. Other observations in these catalysts suggest an irregular change of the surface area with the increase of the milling time. A similar behavior was also observed in the present work in the doped MgO samples, as illustrated in Table II.

The CO₂ adsorption isotherms are very sensitive to the presence of polar groups or ions on the surface of the solid, such as hydroxyl groups.^{36,37} Carbon dioxide adsorption was used to determine changes in the properties of the catalysts (basic site) due to the amorphization process. The results based on isotherms (illustrated in Figure 4) show that the CO₂ adsorption capacity of MgO is affected by the doping and by the mechanical milling treatment. In general, the results show that the mechanical milling treatment contributes to higher CO₂ adsorption capacity. This suggests that the milling process pro-

TABLE II. Specific surface areas (a) of undoped, Y- and Ce-doped MgO milled powders as a function of milling time^(a)

	Milling time / h :		
	1 h	40 h	80 h
	$a / \text{m}^2 \text{g}$		
MgO	136	187	346
MgOY 5 % ^(b)	130	215	114
MgOY 10 % ^(c)	80	250	88
MgOCe 5 % ^(b)	129	57	104
MgOCe 10 % ^(c)	144	106	114

^(a) Specific surface area, a , of samples was done by BET method.

^(b) x_Y and x_{Ce} is 5 %; ^(c) x_Y and x_{Ce} is 10 %.

TABLE III. Acetone conversions and selectivities (at 300 °C) of Ce-doped MgO milled samples (a),(b)

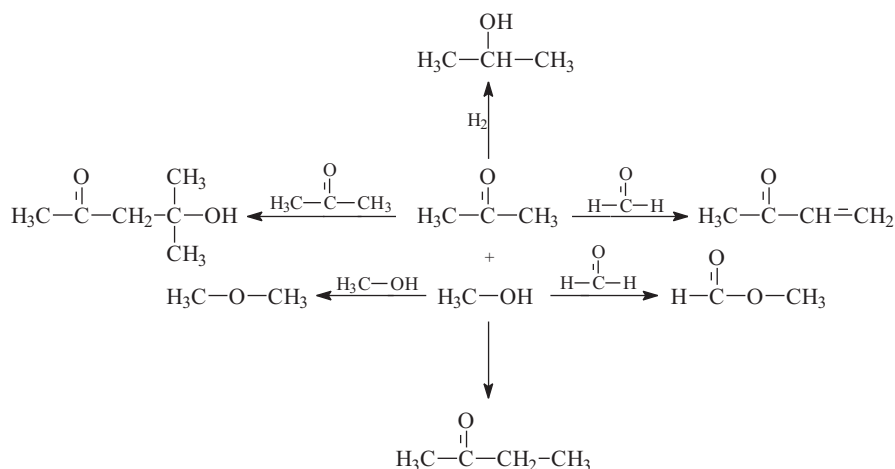
Sample	Conversion / %	Selectivity / %			
		MVK	MEK	IPA	CCP
MgOCe 5 % 1 h (c)	9.7	33.0	4.1	30.1	32.8
MgOCe 5 % 40 h (c)	14.0	24.4	4.7	30.1	40.8
MgOCe 5 % 80 h (c)	13.5	26.2	5.5	29.1	39.2
MgOCe 10 % 1 h (d)	11.0	30.1	4.4	32.5	33.0
MgOCe 10 % 40 h (d)	15.4	25.0	6.4	44.5	24.1
MgOCe 10 % 80 h (d)	11.1	27.8	5.1	40.9	26.2

(a) The values were determined by means of acetone conversion during 4 h of reaction time.

(b) Symbols: MVK, methyl vinyl ketone; MEK, methyl ethyl ketone; IPA, isopropyl alcohol; CCP, cracking and condensation products.

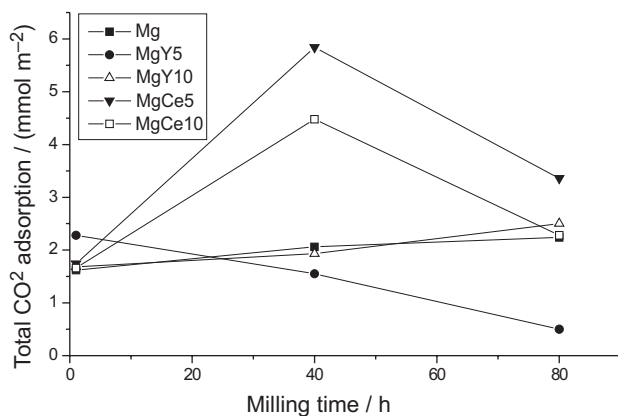
(c) $x_{\text{Ce}} = 5\%$; milling times 1, 40 and 80 h.

(d) $x_{\text{Ce}} = 10\%$; milling times 1, 40, 80 h.



Scheme 1. Formation of main reaction products in aldol condensation between methanol and acetone.

motes easier access of the CO_2 molecule to the adsorption sites of Mg and O. These observations indicate that the basicity is dependent on the milling time, the rare earth promoter and its concentration.

Figure 4. Total amounts of CO_2 adsorption capacity, uptake at 27 °C of undoped and doped MgO samples.

Catalytic Studies

The aldolization reaction between methanol and acetone was studied for each powder sample to acquire more information about their basicity properties. This route allowed catalytic C–C bond formation for the synthesis of α,β -unsaturated compounds (methyl vinyl ketone) by using methanol (as a vinylating agent) for the vinylation of acetone to methyl vinyl ketone (MVK), also forming methyl ethyl ketone (MEK) and isopropyl alcohol (IPA), see Scheme 1.¹² Despite formation of undesirable secondary products (from condensation and cracking processes) during the catalytic conversion of acetone (Figure 5 and Table III), this reaction was taken to be sensitive to the surface characterization of alkaline earth oxide (MgO).

The acetone conversion results obtained with MgO, MgOY ($x = 5\%$) and MgOY ($x = 10\%$) show a relation between the surface area and catalytic activities; the higher the surface area, the higher is acetone conversion.

On the other hand, samples doped with CeO_2 showed higher acetone conversion in catalysts with a lower

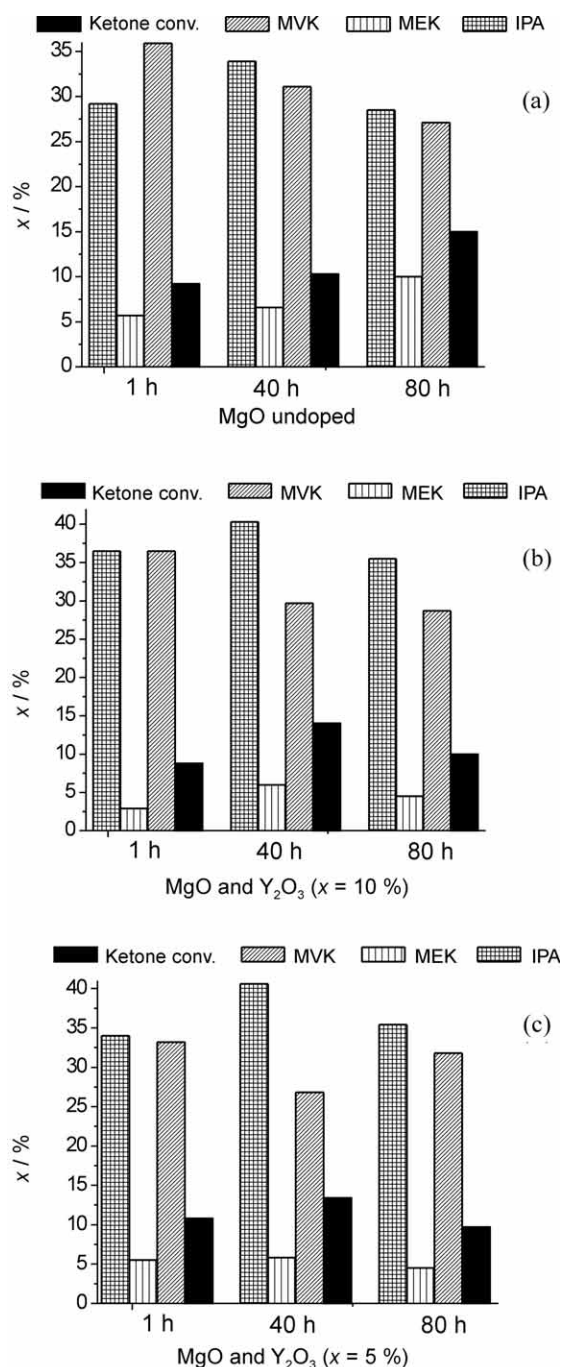


Figure 5. Ketone conversions and selectivity (at 300 °C) for samples of milled powders of undoped MgO and doped MgO-Y₂O₃. The values were determined by means of acetone conversions during 4 h of reaction.

surface area. This result corroborates the behavior of samples in CO₂ adsorption and in the XRD profile. They showed higher CO₂ adsorption and the Mg(OH)₂ peak presence.

The results of acetone conversion observed for all samples indicate that an important requisite to improve the activity is to increase the number of OH groups on the catalyst surface.

The aldolization reaction was used as a probe and allowed monitoring of the basic sites of all samples. It showed varied selectivity in the aldolization reaction. In this process, considerable amounts of isopropyl alcohol and methyl vinyl ketone were formed. According to the data collected in Figure 5, all samples milled for 1 h led to values of MVK selectivity close to the value found for the MgO starting sample. All these samples display values of total and irreversible CO₂ adsorption lower than the ones obtained for the samples milled for 40 h, which favoured IPA selectivity.

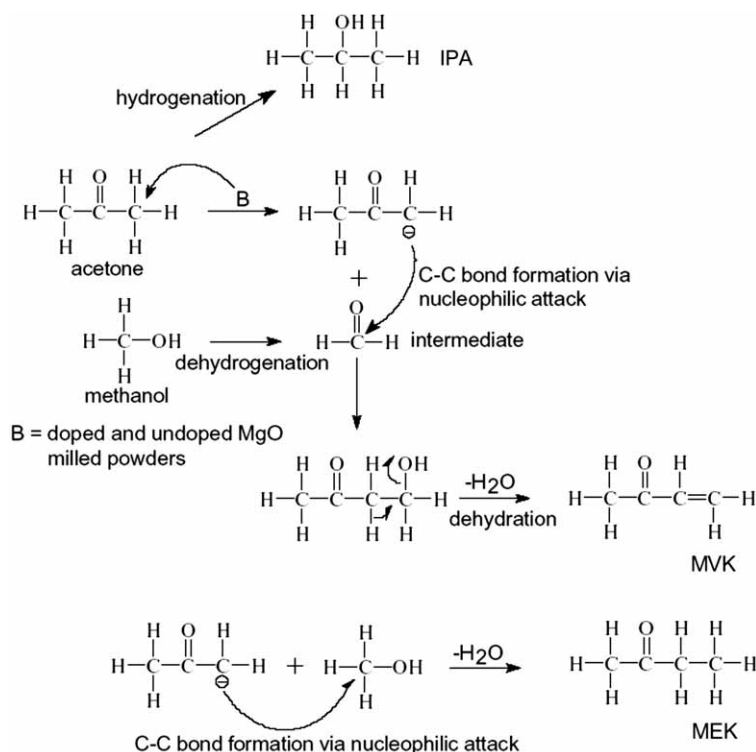
Scheme 2 illustrates the simultaneous events that occur during the aldolization reaction; hydrogenation/dehydrogenation and dehydration. Thus, the role of the basic site strength is to abstract one proton of the acetone molecule to form a carbanion, and this intermediate compound provides the conditions for the C–C bond formation by the condensation process. The carbanion may react with the intermediate product of methanol dehydrogenation, *via* nucleophilic attack, to give MVK. The MEK molecule is formed during the reaction of a second methanol molecule with carbanion. This C–C bond also occurs *via* nucleophilic attack; otherwise, the hydrogenation of acetone molecule leads to IPA. These pathways were previously discussed by several authors,^{38–40} who suggested that the catalytic properties of inorganic magnesium oxide with weak basic sites often differ from those of oxides with stronger basic sites.

These results indicate that the chemical and physical properties of milled MgO samples are dependent on and related to modifications of catalytic basic surfaces.

The herein reported analyses and characterizations of the active surface sites on milled MgO powders provide more information about the catalytic phenomena promoted by surface basicity and hydroxyl groups.

CONCLUSIONS

Analyzing the physical and chemical properties of doped and undoped milled MgO nanostructured powders, one can notice that these materials display properties that differ from those of the same unmilled materials. The photoluminescence and CO₂ chemisorption analyses of alkaline-earth oxides were associated with the monitored structural perturbations in hydroxyl groups and in active basic sites. Structural perturbations are directly related to the type of defects on the nanocrystalline surfaces that are promoted by the amorphization process. The results confirm the ability of the high-energy mechanical milling method to modify the catalytic basic properties or basic strength on catalyst surfaces. Thus, new weak basic sites and stronger basic sites are formed during the milling. Consequently, the sensitivity and selectivity of alkaline-earth oxides may be improved for the catalytic process.



Scheme 2. Formation of isopropyl alcohol (IPA), methyl vinyl ketone (MVK) and methyl ethyl ketone (MEK) over MgO milled powders via dehydrogenation and dehydration processes.

The aldolization reaction requires a surface able to promote the catalysis of hydrogenation/dehydrogenation process, which relies upon the basic sites. These surfaces were substantially affected during the amorphization process.

Acknowledgments. – The authors acknowledge the following Brazilian funding support agencies: FAPESP, CNPq, CAPES and FINEP.

REFERENCES

- V. R. Choudhary and M. Y. Pandit, *Appl. Catal.* **71** (1991) 265–274.
- V. R. Choudhary, V. H. Rane, and S. T. Chaudhari, *Appl. Catal. A Gen.* **158** (1997) 121–136.
- N. E. Fouad, P. Thomasson, and H. Knözinger, *Appl. Catal. A Gen.* **196** (2000) 125–133.
- M. Varga, Á. Molnár, G. Mulas, M. Mohai, I. Bertóti, and G. Cocco, *J. Catal.* **206** (2002) 71–81.
- S. A. El-Molla, M. N. Hammed, and G. A. El-Shobaky, *Mater. Lett.* **58** (2004) 1003–1011.
- V. R. Choudhary and V. H. Rane, *J. Catal.* **130** (1991) 411–422.
- V. R. Choudhary, V. H. Rane, and R. V. Gadre, *J. Catal.* **145** (1994) 300–311.
- P. Thomasson, O. S. Tyagi, and H. Knözinger, *Appl. Catal. A Gen.* **181** (1999) 181–188.
- E. R. Leite, L. P. S. Santos, N. L. V. Carreño, E. Longo, C. A. Paskocimas, J. A. Varela, F. Lanciotti Jr., C. E. M. Campos, and P. S. Pizani, *Appl. Phys. Lett.* **78** (2001) 2148–2150.
- C. C. Koch, *Nanostructured Mater.* **9** (1997) 13–22.
- W. Ueda, T. Yokoyama, Y. Morooka, and T. Ikawa, *J. Chem. Soc., Chem. Commun.* **1** (1984) 39–40.
- N. L. V. Carreño, H. V. Fajardo, A. P. Maciel, A. Valentini, F. M. Pontes, L. F. D. Probst, E. R. Leite, and E. Longo, *J. Mol. Catal. A* **207** (2004) 91–96.
- Powder Diffraction File, Joint Committee on Powders Diffraction Standards, 1989, PDF # 07-0239, 45-0946, 25-1200, and 43-1002.
- E. W. Nuffield, *X-Ray Diffraction Methods*, John Wiley and Sons, New York, 1986, p. 80.
- J. Y. Huang, H. Yasuda, and H. Mori, *J. Am. Ceram. Soc.* **83** (2000) 403–409.
- N. J. Welham, *J. Mater. Res.* **15** (2000) 2400–2407.
- J. Rodríguez-Carvajal, *Physica B Cond. Matter.* **192** (1993) 55–69.
- H. Klug and L. Alexander, *X-Ray Diffraction Procedures*, John Wiley and Sons, New York, 1954, p. 91.
- P. J. Anderson, R. F. Horlock, and J. F. Oliver, *Trans. Faraday Soc.* **61** (1965) 2754–2762.
- R. I. Razouk and R. S. Mikhail, *J. Phys. Chem.* **59** (1955) 636–640.
- E. Longo, J. A. Varela, A. N. Senapeschi, and O. J. Whittemore, *Langmuir* **1** (1985) 456–461.
- M. Boudart, A. Delbouille, E. G. Derouane, V. Indovina, and A. B. Walters, *J. Am. Chem. Soc.* **94** (1972) 6622–6630.
- P. R. de Lucena, F. M. Pontes, C. D. Pinheiro, E. Longo, P. S. Pizani, S. Lázaro, A. G. Souza, and I. M. G. dos Santos, *Cerâmica* **50** (2004) 138–144.

24. M. Anpo, M. Kondo, C. Louis, M. Che, and S. Coluccia, *J. Am. Chem. Soc.* **111** (1989) 8791–8799.
25. M. Anpo, S. Higashimoto, M. Matsuoka, N. Zhanpeisov, Y. Shioya, S. Dzwigaj, and M. Che, *Catal. Today* **78** (2003) 211–217.
26. M. Sterrer, O. Diwald, E. Knozinger, P. V. Sushko, and A. L. Shluger, *J. Phys. Chem. B* **106** (2002) 12478–12482.
27. Y. Kawaguchi, *Solid State Commun.* **117** (2000) 17–20.
28. J. Zhang and L. Zhang, *Chem. Phys. Lett.* **363** (2002) 293–297.
29. E. R. Leite, N. L. V. Carreño, L. P. S. Santos, J. H. Rangel, L. E. B. Soledade, E. Longo, C. E. M. Campos, F. Lanciotti Jr., P. S. Pizani, and J. A. Varela, *Appl. Phys. A Mater.* **73** (2001) 567–569.
30. P. S. Pizani, E. R. Leite, F. M. Pontes, E. C. Paris, J. H. Rangel, E. J. H. Lee, E. Longo, P. Delega, and J. A. Varela, *Appl. Phys. Lett.* **77** (2000) 824–826.
31. M. Anpo, Y. Yamada, Y. Kubokawa, S. Coluccia, A. Zecchina, and M. Che, *J. Chem. Soc., Faraday Trans. 1* **84** (1988) 751–764.
32. M. Anpo, Y. Yamada, Y. Kubokawa, S. Coluccia, A. Zecchina, and M. Che, *J. Chem. Soc., Faraday Trans. 1* **85** (1989) 609–620.
33. Y. Kawaguchi, *Phys. Rev. B* **54** (1996) 9721–9725.
34. H. Yoshida, T. Tanaka, T. Funabiki, and S. Yoshida, *Faraday Trans.* **90** (1994) 2107–2111.
35. H. Kawakami and S. Yoshida, *J. Chem. Soc., Faraday Trans. 2* **80** (1984) 921–932.
36. N. O. Lemcoff and K. S. W. Sing, *J. Colloid Interf. Sci.* **61** (1977) 227–232.
37. J. Sanchez Valente, F. Figueras, M. Gravelle, P. Kumbhar, J. Lopez, and J. P. Besse, *J. Catal.* **189** (2000) 370–381.
38. H. V. Fajardo, L. F. D. Probst, A. Valentini, N. L. V. Carreño, A. P. Maciel, E. R. Leite, and E. Longo, *J. Braz. Chem. Soc.* **16** (2005) 607–613.
39. M. Huang, P. A. Zielinski, J. Moulod, and S. Kaliaguine, *Appl. Catal. A Gen.* **118** (1994) 33–49.
40. E. Iglesia, D. G. Barton, J. A. Biscardi, M. J. L. Gines, and S. L. Soled *Catal. Today* **38** (1997) 339–360.

SAŽETAK

Amorfizacijski efekti na bazična mjesta nanometarskih čestica magnezijeva oksida

Neftalí Lenin Villarreal Carreño, David Keyson, Marcia Tsuyama Escote, Edson Roberto Leite, Elson Longo, Humberto Vieira Fajardo, Luiz Fernando Dias Probst, Antoninho Valentini, Miryam Rincón Joya i Paulo Sergio Pizani

Opisana je katalitička aktivnost bazičnih mjesta nanokristalnih čestica magnezijeva oksida dopiranog elementima rijetkih zemalja na stvaranje veze C–C u α,β -nezasićenom spoju (metil-vinil-keton). Nedopirani i dopirani uzorci MgO pripremljeni su visokoenergijskim mehaničkim mljevenjem komercijalnih praškastih uzoraka magnezijeva, itrijeva i cerijeva oksida. Na katalitičku aktivnost i površinsku bazičnost tih spojeva izrazito utječu dopiranje i vrijeme mehaničkog mljevenja (proces amorfizacije). Mljevenje dovodi do stvaranja nanokristalnih materijala. Utjecaj mehaničke obrade spomenutih spojeva istražen je adsorpcijom N₂ (BET), difrakcijom rentgenskih zraka, mikroskopijom TEM, adsorpcijom CO₂ i fotoluminescencijom pri sobnoj temperaturi. Velike promjene polarnih grupa, poput hidroksilne, na površini krutine direktno su povezane s opaženom fotoluminescencijom.